

# Spontaneous Synchronization in Cellular Circadian Clocks

Yuelong Li

December 2022

## 1 Introduction

Beyond the simple one direction transcription and translation flow, proteins translated by ribosome in the cytoplasm can be imported into the nucleus, and interact with the DNA, forming complex cellular dynamics. In a previous paper by Wang and Peskin [1], a four species model was put forth describing the cellular dynamics governing circadian rhythms through the formation of non-linear phase oscillator.

In this paper I will generalize this dynamics into the regime of multiple interacting cells. Their cellular interaction is based on the assumption that some of the molecules governing the circadian cycle will diffuse into the blood stream, and some molecules in the blood stream will also diffuse into cell cytoplasm. The two diffusion process happen at different rates based on different concentrations of molecules inside and outside the cells, hence causing a kind of "exchange" which may give rise to synchronization. Then I will make attempts to simulate and theorize the emergent behaviors in an interacting system of cellular clocks such as synchronization, or collective damping.

## 2 Single Cell Model

In a single cell oscillator, our model consists of four species of molecules, which are respectively: mRNA in nucleus ( $m_n$ ), mRNA in cytoplasm ( $m_c$ ), protein in cytoplasm ( $p_c$ ), and protein in the nucleus ( $p_n$ ). mRNA are created through DNA transcription and enter into the cytoplasm through diffusion at a rate of  $\gamma_m$  (prb/hr), proteins are made in the cytoplasm and enter into the nucleus also through diffusion at a rate of  $\gamma_p$  (prb/hr). While concentration of mRNA molecules drive the transcription at a rate of  $\beta$ , proteins in the nucleus inhibits the transcription by binding to the DNA sites at a rate of  $\xi$  (prb/hr) and unbinding at a rate of  $\eta$  (prb/hr). Additionally, mRNA in the cytoplasm spontaneously degrade at a rate of  $\delta_m$  and proteins in the nucleus at a rate of  $\delta_p$ .

| Reaction # | Name          | Probability/Time | Result                            |
|------------|---------------|------------------|-----------------------------------|
| 1          | Transcription | $\alpha P_0$     | $\#(m_n) \rightarrow \#(m_n) + 1$ |
| 2          | Export        | $\gamma_n m_n$   | $\#(m_n) \rightarrow \#(m_n) - 1$ |
|            |               |                  | $\#(m_c) \rightarrow \#(m_c) + 1$ |
| 3          | Degradation n | $\gamma_c m_c$   | $\#(m_c) \rightarrow \#(m_c) - 1$ |
| 4          | Translation   | $\beta m_c$      | $\#(p_c) \rightarrow \#(p_c) + 1$ |
| 5          | Import        | $\gamma_p p_c$   | $\#(p_c) \rightarrow \#(p_c) - 1$ |
|            |               |                  | $\#(p_n) \rightarrow \#(p_n) + 1$ |
| 6          | Degradation p | $\delta_p p_n$   | $\#(p_n) \rightarrow \#(p_n) - 1$ |

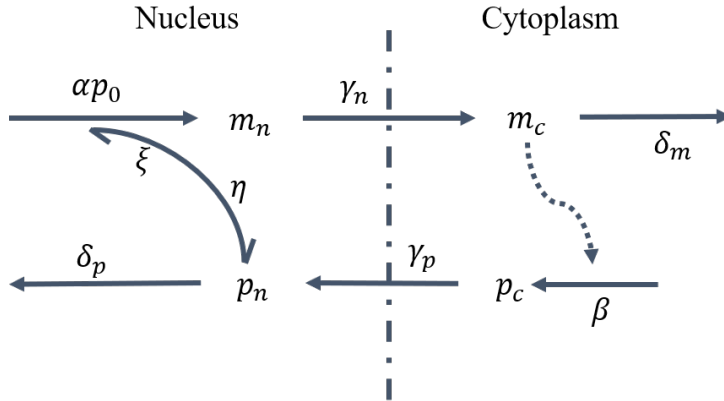


Figure 1: Molecular oscillator in a single cell

## 2.1 Protein Binding

$m_p$  is only created when there are no inhibitory proteins bound to the DNA. To the probability per unit time that this process happens, we will also need the probability that there are no DNA bound to any of the DNA sites.  $r \in \mathbb{Z}$  describes the number of sites there are on the DNA for inhibitory proteins to bind. Let  $k_1, k_2$  be the macro rate constants corresponding to the micro rate constants  $\xi, \eta$ , with relations:

$$k_1[A][B] = \frac{d}{dt}[AB],$$

$$\xi \#(A)\#(B) = \frac{d}{dt}\#(AB).$$

By dividing both sides of the macro rate constant by the nucleus volume  $V$ , we get:

$$\xi = \frac{k_1}{V}.$$

Similarly:

$$\begin{aligned} k_2[AB] &= \frac{d}{dt}[A] = \frac{d}{dt}[B], \\ \eta \#(AB) &= \frac{d}{dt}\#(A) = \frac{d}{dt}\#(B). \\ \Rightarrow \eta &= k_2. \end{aligned}$$

So if we set  $K = \frac{k_2}{k_1}$ , then  $\frac{\eta}{\xi} = KV$ .

If we denote by  $P_l$  the probability that  $l$  sites are occupied, then  $\alpha P_0$  corresponds to the transcription rate. To find  $P_0$ , we consider the fast probabilistic equilibrium between state  $P_l$  and  $P_{l+1}$ , satisfying:

$$\xi(r-l)(p_n - l)P_l = \eta(l+1)P_{l+1},$$

notice in this equation  $r-l$  corresponds to the number of empty DNA sites for binding,  $p_n - l$  is the remaining number of proteins available for binding. On the right side,  $l+1$  correspond to the number of bound DNA sites available for decomposition. Through manipulation of the relation, we can express  $P_l$  in terms of  $P_0$  for all  $l \in [\min(r, \#(p_n))]$ . In our case we can assume  $p_n$  to be large and there will always be proteins available for binding, so that  $l$  can run from 0 to  $r$ .

Then normalizing the total sum of probabilities to 1 yields (for large  $p_n$ ):

$$P_0 = \frac{1}{\sum_{l=0}^r \binom{r}{l} \binom{p_n}{l} l! \left(\frac{\xi}{\eta}\right)^l} = \frac{1}{\sum_{l=0}^r \binom{r}{l} p_n^l \left(\frac{\xi}{\eta}\right)^l} = \frac{1}{(1 + p_n/KV)} = \frac{K}{(K + p_n/V)}. \quad (1)$$

## 2.2 Continuous time model

Now we have the value of  $P_0$  in relation to  $p_n$ , we can write down the differential equations governing the molecular population. We will be using directly the molecule number instead of concentration in this paper, as they are more intuitive to work with, and cellular dynamics naturally involve small number of dynamics. But even though the molecule numbers are small, we will only be considering the molecule numbers under continuous change to simplify calculations. The previous paper [1] has provided thorough comparisons between the results obtained from stochastic and continuous models.

$$\begin{aligned} \frac{dm_n}{dt} &= \alpha \left( \frac{K}{K + \frac{p_n}{V}} \right)^r - \gamma_m m_n \\ \frac{dm_c}{dt} &= \gamma_m m_n - \delta_m m_c \\ \frac{dp_c}{dt} &= \beta m_c - \gamma_p p_c \\ \frac{dp_n}{dt} &= \gamma_p p_c - \delta_p p_n. \end{aligned}$$

The critical point of this system occurs when all derivatives go to 0. Then we obtain:  $\alpha \left( \frac{K}{K + \frac{p_n}{V}} \right)^r = \gamma_m m_n = \delta_m m_c = \frac{\delta_m}{\beta} \gamma_p p_c = \frac{\delta_m}{\beta} \delta_p p_n$ . Thus giving the equilibrium condition for  $p_n$ :

$$\begin{aligned} \alpha \left( \frac{K}{K + \frac{p_n}{V}} \right)^r &= \frac{\delta_m}{\beta} \delta_p p_n. \\ \Rightarrow \alpha \beta \left( \frac{K}{K + \frac{p_n}{V}} \right)^r &= \delta_m \delta_p p_n. \end{aligned} \quad (2)$$

Take the solution to this expression to be  $p_{n0}$ . Around the equilibrium point, we shall approximate the non-linear term in  $\frac{dm_n}{dt}$  by:

$$\frac{\partial}{\partial p_n} \left( \alpha \left( \frac{K}{K + \frac{p_n}{V}} \right)^r \right) = -\frac{r \delta_p \delta_m}{\beta} \left( \frac{p_{n0}/V}{K + p_{n0}/V} \right) \equiv -a.$$

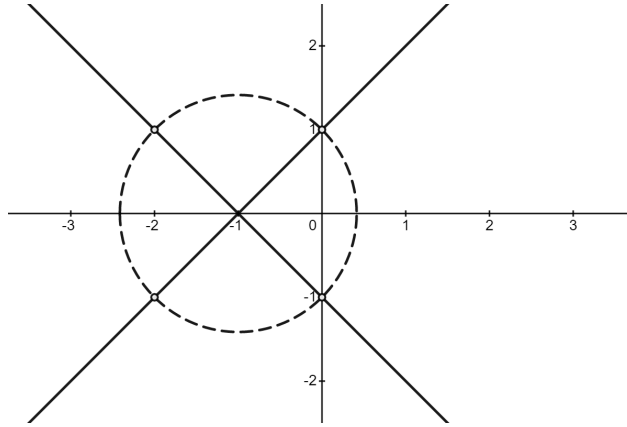


Figure 2: The possible values of  $\lambda$  (solid lines) and the circle (dashed line) of radius  $G^{\frac{1}{4}}$  that crosses it at the solutions of the characteristic.

Then we obtain for  $\tilde{x} = x - x_0$ :

$$\begin{aligned}\frac{d\tilde{m}_n}{dt} &= a\tilde{p}_n - \gamma_m \tilde{m}_n \\ \frac{d\tilde{m}_c}{dt} &= \gamma_m \tilde{m}_n - \delta_m \tilde{m}_c \\ \frac{d\tilde{p}_c}{dt} &= \beta \tilde{m}_c - \gamma_p \tilde{p}_c \\ \frac{d\tilde{p}_n}{dt} &= \gamma_p \tilde{p}_c - \delta_p \tilde{p}_n.\end{aligned}$$

We shall let  $\gamma_m = \delta_m = \gamma_p = \delta_p = \nu$ . Then, characteristic of this linear expression satisfy:

$$\left(\frac{\lambda}{\nu} + 1\right)^4 = -\frac{a\beta}{\nu^2} = -r\nu^2 \left(\frac{p_{n0}/V}{K + p_{n0}/V}\right) \equiv -G.$$

For  $\left(\frac{\lambda}{\nu} + 1\right)^4$  to equal a negative real number,  $\left(\frac{\lambda}{\nu} + 1\right)$  must make 45 degree angles with the real axis in the complex plane. So for  $\lambda$  to have positive real part, it must hold that  $\left|\frac{\lambda}{\nu} + 1\right| \geq \sqrt{1+1} = \sqrt{2}$ , with  $|G| = \left|\left(\frac{\lambda}{\nu} + 1\right)^4\right| \geq \sqrt{2}^4 \geq 4$ . Then

$$G = r \left(\frac{p_{n0}/V}{K + p_{n0}/V}\right) \geq 4.$$

Because  $\frac{p_{n0}/V}{K + p_{n0}/V} < 1$ , we obtain  $r > 4$ . We shall take  $r = 5$ . Additionally, in the special case that  $G = 4$ ,  $(\frac{\lambda}{\nu} + 1)$  solves exactly to be  $\lambda = i\nu$ . This implies the oscillation cycle will have a relatively constant amplitude, with an angular frequency of  $\nu$ .

Because we want oscillation of 24 hours corresponding to the regular circadian rhythm, we shall take  $\nu = \frac{2\pi}{24}$ . On the other hand, due to the existence of non-linear terms in the actual differential equation, the solution are not perfect ellipsoids around the equilibrium points, and setting  $\nu = \frac{2\pi}{22}$  gives a oscillator period of 24 hours, as we will see in the simulations. Now with  $G = 4$ , we may solve for  $K$ , in terms of  $p_{n0}$ :

$$K = \left(\frac{r}{4} - 1\right) p_n^0 / V.$$

Additionally, we take  $\beta = 10\text{h}^{-1}$  from the previous paper and  $V = 0.5(\text{pL})$  as a small arbitrary number to yield a reasonable value for  $\alpha$ . With  $p_n^0$  (the equilibrium point) given, we may solve for a value of  $\alpha$  based on expression (2):

$$\alpha = \frac{\delta_m \delta_p p_n^0}{\beta} \left( \frac{K + p_n^0/V}{K} \right)^r.$$

We take  $p_{n0} = 500$ , so that the oscillation will always leave a large enough  $p_n$  for expression (1) to hold.

## 2.3 Simulation

With initialization conditions  $m_n^0 = 10.9$ ,  $m_c^0 = 1.88$ ,  $p_n^0 = 500$ ,  $p_c^0 = 250$  (these are initial values, not critical point values), and the following parameter initialization:

```
nu = 2*math.pi/22
gm = nu
dm = nu
gp = nu
dp = nu
r = 5
b = 10
V=0.1
pn0 = 500
K=(r/4-1)*pn0*V+1 #K = 63.5
a=dm*dp*pn0*((K+pn0/V)/K)**r/b #alpha => a = 5374068
```

we use an RK4 integrator implemented in python to obtain the following result.

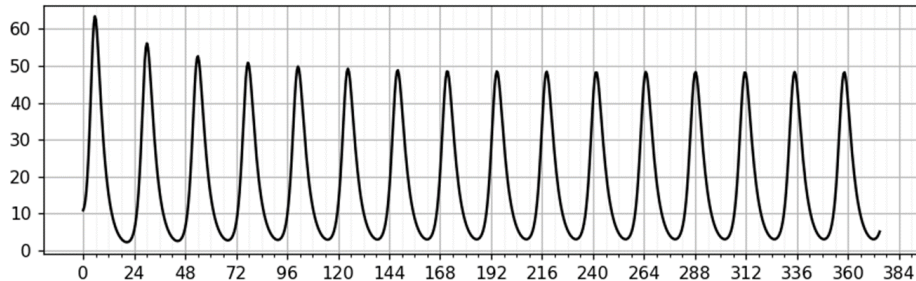


Figure 3: Molecular count for  $m_n$  versus time (in hours elapsed) for initial conditions given, which can be seen to stabilize into a fixed orbit.

## 2.4 Validation

We plot the total number of proteins  $p = p_n + p_c$  and take its derivative. We expect to see  $\frac{dp}{dt} = \beta m_c - \delta_p p_n$ . The expected rate of change of  $p_n$  and its actual rate of change match when integrator precision is set to  $10^{-35}$ .

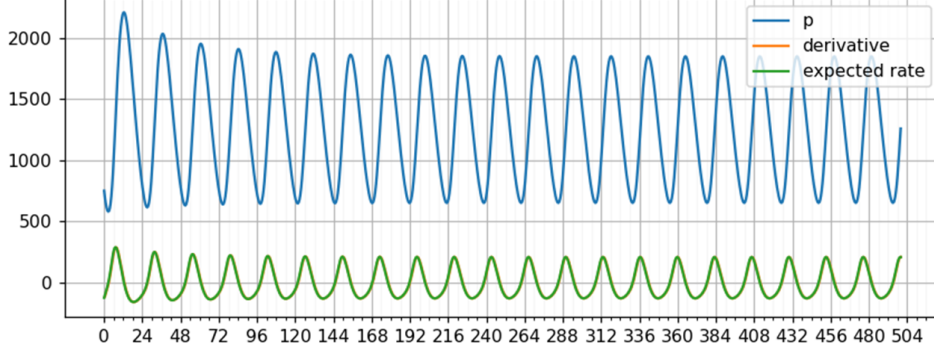


Figure 4: Total number of proteins (blue) and its derivative (orange, covered) vs time (hrs), which matches the expected rate of change (green).

### 3 Multi Cell Model

Now we introduce the augmented model including multiple cells and their interactions.

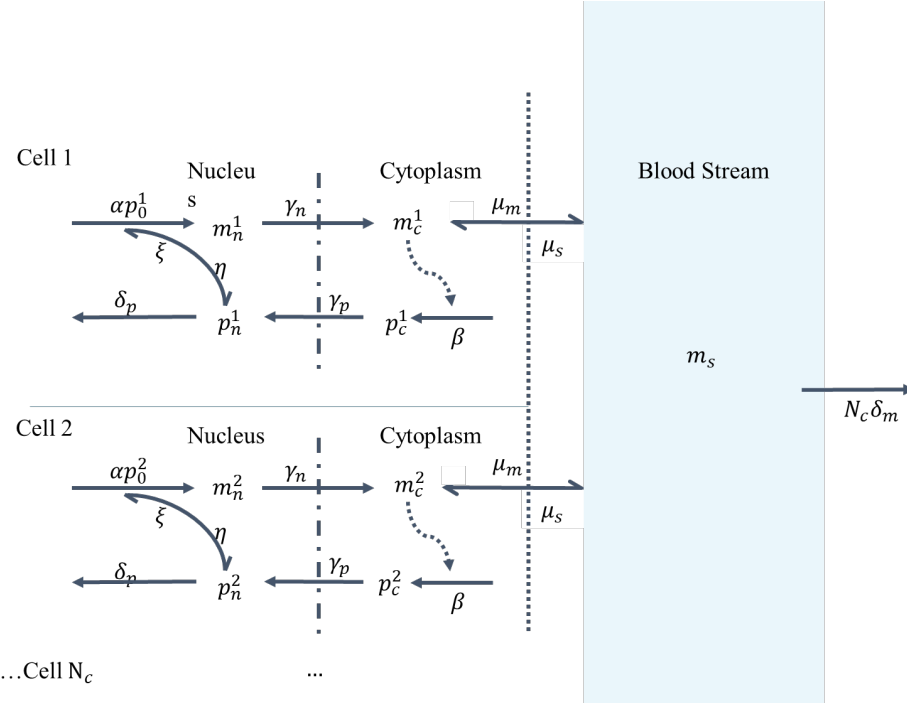


Figure 5: The molecular flow with additional parameters  $N_c$  : cell count,  $m_s$ : blood mRNA level,  $\mu_m$ : membrane diffusion,  $\mu_s$ : membrane infusion

In the multi-cell model, we attach all cells to a blood stream, and assume that cytoplasm mRNA  $m_c$  can travel from membrane into the blood stream or vice versa through diffusion. The two micro rate constants are  $\mu_m$  and  $\mu_s$  respectively. The model essentially considers all cells to be connect to a single vertex of blood stream, forming a star shape in their connection graph. This is valid because the production rate of mRNA is slow (on the scale of hours)

| Reaction # | Name               | Probability/Time   | Result                                |
|------------|--------------------|--------------------|---------------------------------------|
| 1          | Transcription      | $\alpha p_0^i$     | $\#(m_n^i) \rightarrow \#(m_n^i) + 1$ |
| 2          | Export             | $\gamma_n m_n^i$   | $\#(m_n^i) \rightarrow \#(m_n^i) - 1$ |
|            |                    |                    | $\#(m_c^i) \rightarrow \#(m_c^i) + 1$ |
| 3          | <b>Diffusion</b>   | $\mu_c m_c^i$      | $\#(m_c^i) \rightarrow \#(m_c^i) - 1$ |
|            |                    |                    | $\#(m_s) \rightarrow \#(m_s) + 1$     |
| 4          | Translation        | $\beta m_c^i$      | $\#(p_c^i) \rightarrow \#(p_c^i) + 1$ |
| 5          | Import             | $\gamma_p p_c^i$   | $\#(p_c^i) \rightarrow \#(p_c^i) - 1$ |
|            |                    |                    | $\#(p_n^i) \rightarrow \#(p_n^i) + 1$ |
| 6          | Degradate p        | $\delta_p p_n^i$   | $\#(p_n^i) \rightarrow \#(p_n^i) - 1$ |
| 7          | <b>Infusion</b>    | $\mu_s m_s$        | $\#(m_c^i) \rightarrow \#(m_c^i) + 1$ |
|            |                    |                    | $\#(m_s) \rightarrow \#(m_s) - 1$     |
| 8          | <b>Degradate n</b> | $N_c \delta_m m_s$ | $\#(m_s) \rightarrow \#(m_s) - 1$     |

compared to the blood circulation rate, so it is not necessary to consider their locality in the blood stream.

We will keep all the previously specified constant with the same values. Additionally, cells no longer degrade mRNA molecules inside the cytoplasm, but instead diffuse them into the blood stream, where they are degraded at a rate of  $N_c \delta_m m_s$ . Note that the original constant  $\delta_m$  is scaled by a factor of  $N_c$ , as there are  $N_c$  cells exporting mRNA molecules. To account for cellular exchange, we introduce parameter  $\epsilon$  called the exchange rate, and let  $\mu_n = \epsilon + \delta_m$ ,  $\mu_p = \epsilon$ . This way if synchronization is reached, the additional export of  $\epsilon m_c$  should cancel out the import of  $\epsilon m_s$ , leaving equivalently a degradation rate of  $\delta_m m_c$ . This way the individual cells will keep their dynamics discussed in section 2 when synchronized, and hence the circadian period of 24 hours. The new differential equations governing the cellular dynamics are:

$$\begin{aligned} \frac{dm_n^i}{dt} &= \alpha \left( \frac{K}{K + \frac{p_n^i}{V}} \right)^r - \gamma_m m_n^i \\ \frac{dm_c^i}{dt} &= \gamma_m m_n^i - \mu_m m_c^i + \mu_s m_s \\ \frac{dp_c^i}{dt} &= \beta m_c^i - \gamma_p p_c^i \\ \frac{dp_n^i}{dt} &= \gamma_p p_c^i - \delta_p p_n^i \\ \frac{dm_s}{dt} &= \sum_{i=1}^{N_c} \mu_c m_c^i - N_c \mu_s m_s - N_c \delta_m m_s \end{aligned}$$

Keep previous parameters unchanged:  $\alpha, \beta, K, V, \gamma_m, \delta_m, \gamma_p, \delta_p$ . Additional parameters,  $\mu_c = \delta_m + \epsilon$ ,  $\mu_s = \epsilon$ , where  $\epsilon$  is the exchange rate.

### 3.1 Multi-cell simulation

To know the starting state of each cells, we sample their molecule counts from a phase instant from the stabilized solutions obtained for a single cell. To sample a circadian cycle, we start at  $t > 240$  and find  $t$  corresponding to the first and second minima of  $m_n$  concentration.

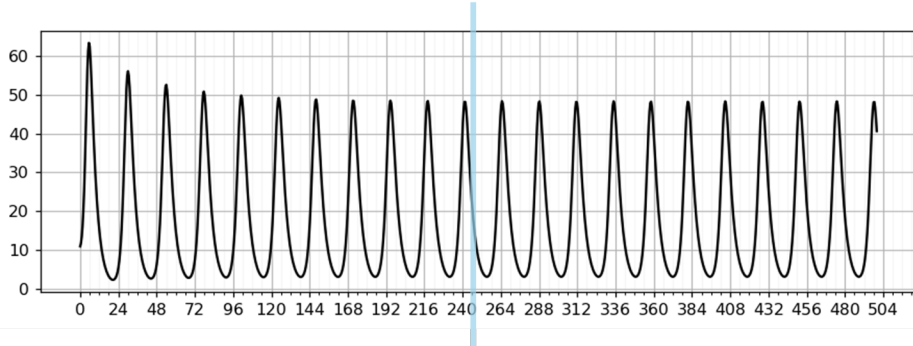


Figure 6: We sample for a single circadian cycle for  $t > 240$ , where the orbits have stabilized

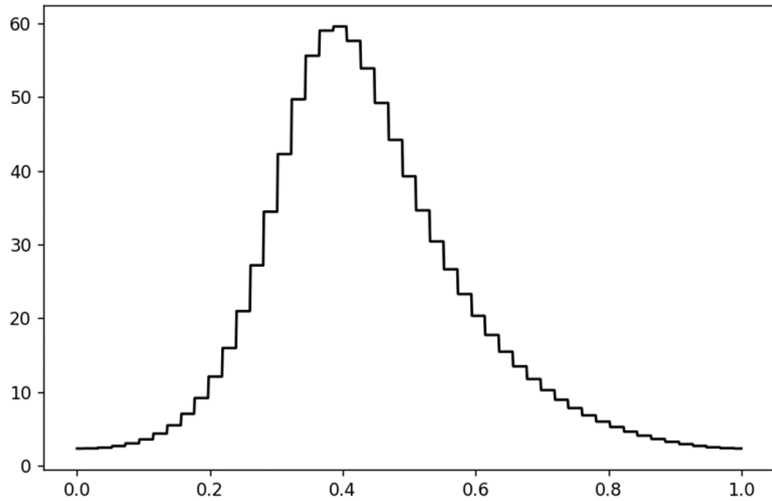
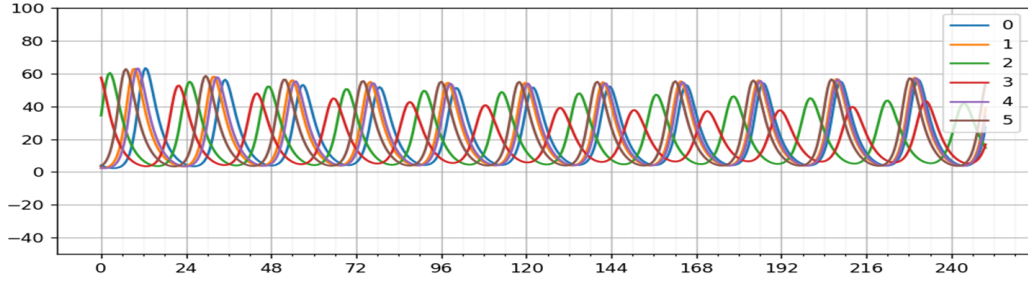


Figure 7:  $m_n$  v.s.  $t$  sampled over a period of dynamic equilibrium

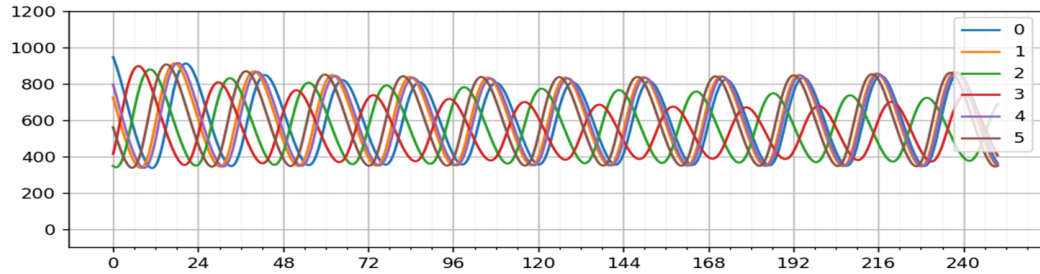
We then take the solution orbit  $\mathbf{S} : [0, 2\pi] \rightarrow \mathbf{R}^4$  between these two timestamps as a single cycle, rescaled to  $\phi \in [0, 2\pi]$ . Next we randomize a list of  $\{\phi_0^i\}$  from the uniform distribution between  $[0, 2\pi]$ . The initial conditions of each cells correspond to  $\mathbf{S}(\phi_0^i)$ .

For a 5 cell system, with  $\epsilon = 2/22$ , we obtain the result in **figure 8**. It can be observed that although slowly, the cellular concentrations are entering into phase coherence. After  $t > 500$ , the cellular phases are mostly synchronized. The blood mRNA of this 5 cell system are as shown in **figure 9**, where we can see that oscillation amplitude of  $m_s$  rises as the system enters into synchronization.

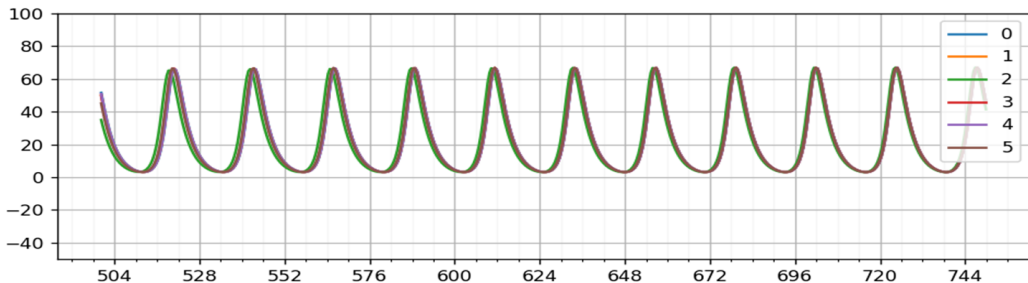
We continue the simulation to a 100 cell system, with  $\epsilon = 1/11$ ,  $\mu_s = \epsilon$ ,  $\mu_c = \delta_m + \epsilon$ ,  $\nu = \frac{2\pi}{11}$ . The resultant orbits between  $t = 0$  and  $t = 250$  are shown in **figure 11**. We also compare  $m_s$  to  $m_c^i$  in **figure 10**, where  $m_s$  seems to oscillate within the phase space volume occupied by  $m_c^i$ .



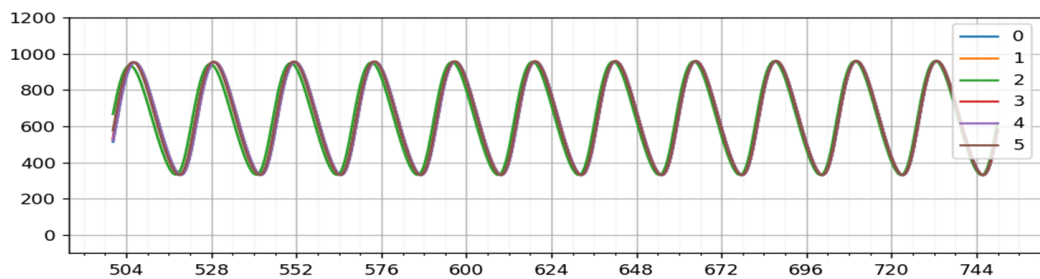
(a)  $m_n^i$  v.s.  $t$ , time between 0 and 250



(b)  $p_n^i$  v.s.  $t$ , time between 0 and 250

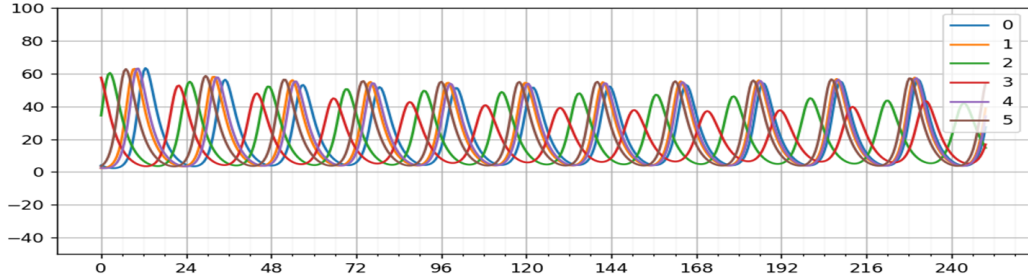


(c)  $m_n^i$  v.s.  $t$ , time between 500 and 750

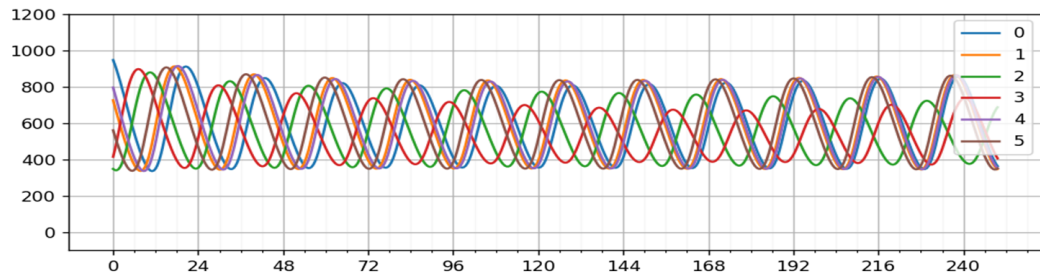


(d)  $p_n^i$  v.s.  $t$ , time between 500 and 750

Figure 8: Simulation result - 5 cells,  $\epsilon = 2/22$ ,  $\mu_c = \delta_m + \epsilon$ ,  $\mu_s = 1 \neq \epsilon$ .

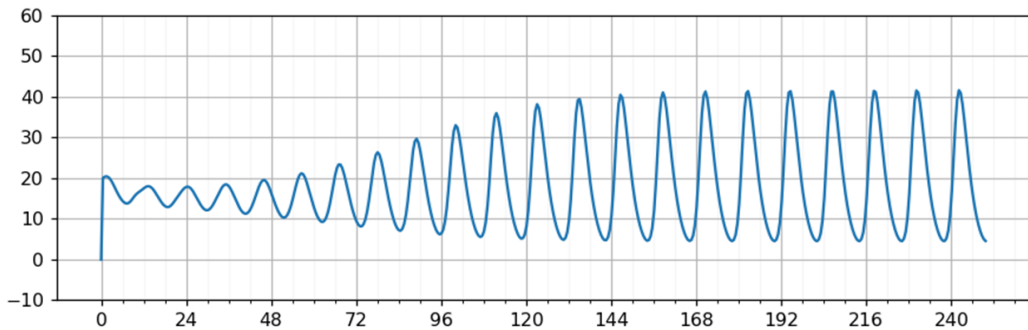


(a)  $m_s$  v.s.  $t$ , time between 0 and 250



(b)  $m_s$  v.s.  $t$ , time between 250 and 750

Figure 9: Simulation result - 5 cells,  $\epsilon = 2/22$ ,  $\mu_c = \delta_m + \epsilon$ ,  $\mu_s = 1 \neq \epsilon$ .



(a)  $m_s$  v.s.  $t$

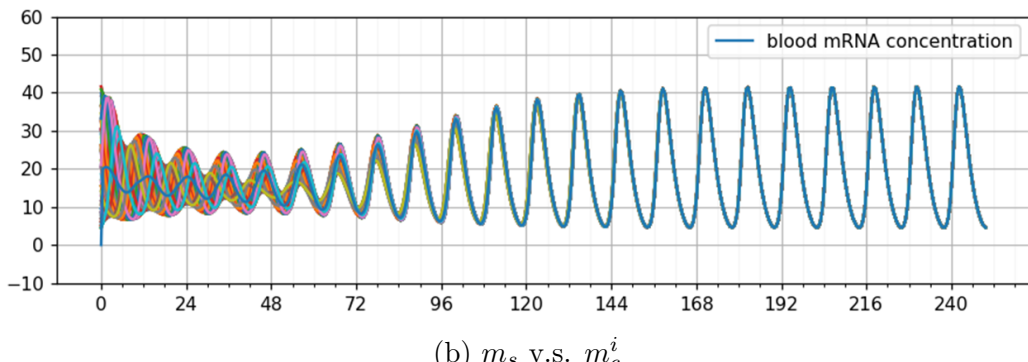
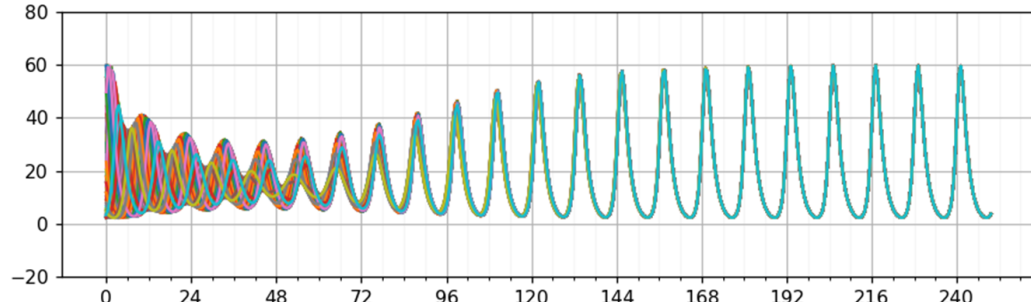
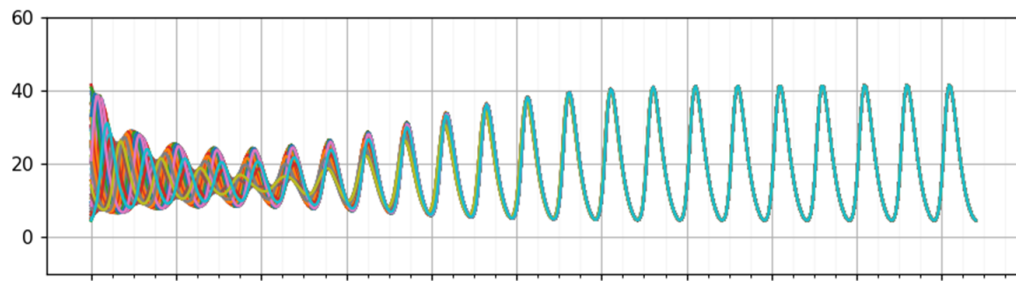


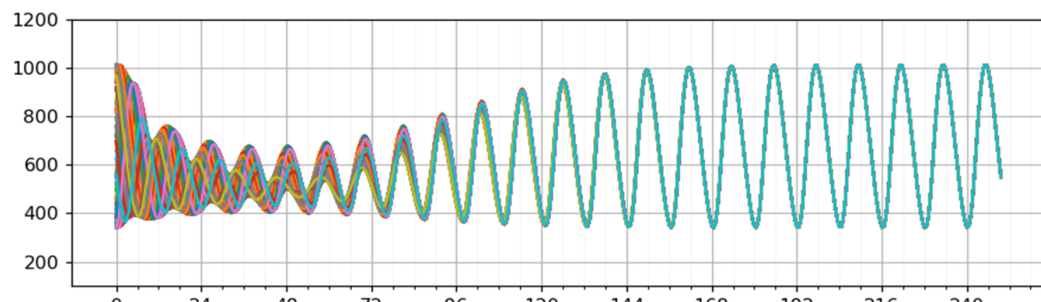
Figure 10:  $m_s$  comparison - 100 cells,  $\epsilon = 2/22$ ,  $\mu_c = \delta_m + \epsilon$ ,  $\mu_s = 1 \neq \epsilon$ .



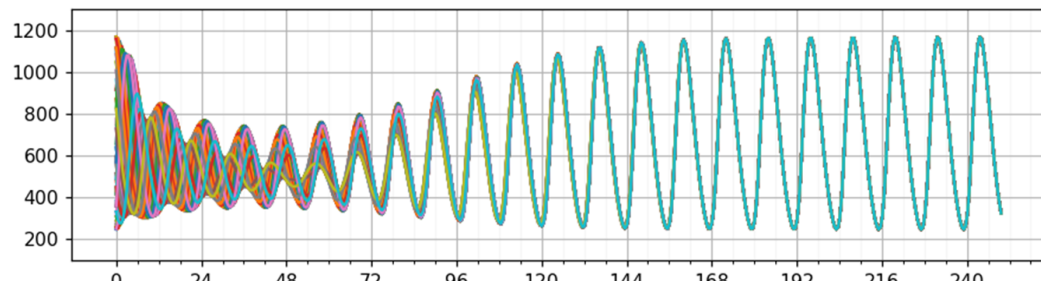
(a)  $m_n^i$  v.s.  $t$



(b)  $m_c^i$  v.s.  $t$



(c)  $p_n^i$  v.s.  $t$



(d)  $p_c^i$  v.s.  $t$

Figure 11: Simulation result - 100 cells,  $\epsilon = 1/11$ ,  $\mu_c = \delta_m + \epsilon$ ,  $\mu_s = \epsilon$ ,  $\nu = 2\pi/11$ .

## 4 Mean Flow Theory

We want to explore in this section possible ways to explain and predict the emerging patterns such as synchronization and collective damping in the cellular system. The original equations of the system are:

$$\begin{aligned}\frac{dm_n^i}{dt} &= \alpha \left( \frac{K}{K + \frac{p_n^i}{V}} \right)^r - \gamma_m m_n^i \\ \frac{dm_c^i}{dt} &= \gamma_m m_n^i - \mu_m m_c^i + \mu_s m_s \\ \frac{dp_c^i}{dt} &= \beta m_c^i - \gamma_p p_c^i \\ \frac{dp_n^i}{dt} &= \gamma_p p_c^i - \delta_p p_n^i \\ \frac{dm_s}{dt} &= \sum_{i=1}^{N_c} \mu_c m_c^i - N_c \mu_s m_s - N_c \delta_m m_s\end{aligned}$$

which involves  $4N_c + 1$  terms. For  $N_c \gg 1$  solving it directly would be difficult. Inspired by mean-field theory in physics, we seek to reduce it to a set of 5 equations by taking their averages for  $i \in [N_c]$ . Then  $x_i \rightarrow \langle x \rangle$  for all the dynamic variables. The summation term in  $\frac{dm_s}{dt}$  is already averaging over  $m_c$ . So we obtain:

$$\begin{aligned}\frac{d\langle m_n \rangle}{dt} &= \frac{1}{N_c} \sum_{i=1}^{N_c} \alpha \left( \frac{K}{K + \frac{p_n^i}{V}} \right)^r - \gamma_m \langle m_n \rangle \\ \frac{d\langle m_c \rangle}{dt} &= \gamma_m \langle m_n \rangle - \mu_m \langle m_c \rangle + \mu_s m_s \\ \frac{d\langle p_c \rangle}{dt} &= \beta \langle m_c \rangle - \gamma_p \langle p_c \rangle \\ \frac{d\langle p_n \rangle}{dt} &= \gamma_p \langle p_c \rangle - \delta_p \langle p_n \rangle \\ \frac{d\langle m_s \rangle}{dt} &= N_c \mu_c \langle m_c \rangle - N_c \mu_s m_s - N_c \delta_m m_s.\end{aligned}$$

Unfortunately  $p_n^i$  in the first expression cannot be reduced due to non-linearity. However, we can take Taylor-expansion of each  $\left( \frac{K}{K + \frac{p_n^i}{V}} \right)^r$  around  $\langle p_n \rangle$ . Then:

$$\begin{aligned}\frac{1}{N_c} \sum_{i=1}^{N_c} \alpha \left( \frac{K}{K + \frac{p_n^i}{V}} \right)^r &= \alpha \left( \frac{K}{K + \frac{\langle p_n \rangle}{V}} \right)^r + \frac{\alpha}{N_c} \frac{\partial}{\partial p_n} \left( \left( \frac{K}{K + \frac{p_n^i}{V}} \right)^r \right) \sum_{i=1}^{N_c} (p_n^i - \langle p_n \rangle) \\ &\quad + \frac{\alpha}{N_c} \frac{\partial^2}{\partial p_n^2} \left( \left( \frac{K}{K + \frac{p_n^i}{V}} \right)^r \right) \sum_{i=1}^{N_c} \frac{(p_n^i - \langle p_n \rangle)^2}{2} + \dots \\ &= \alpha \left( \frac{K}{K + \frac{\langle p_n \rangle}{V}} \right)^r + \frac{\alpha r(r+1)}{2K^2 V^2} \left( \frac{K}{K + \langle p_n \rangle / V} \right)^{(r+2)} \sigma_{pn}^2.\end{aligned}$$

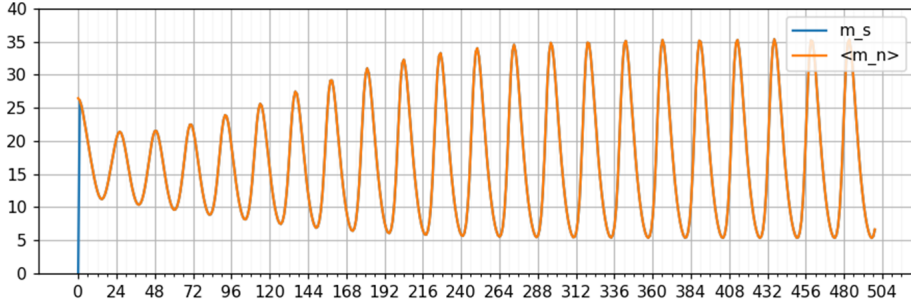


Figure 12: Comparison between  $m_s$  vs  $t$  (blue) and  $\langle m_c \rangle$  vs  $t$  (orange) with  $N_c = 100, \nu = \frac{2\pi}{22}, \epsilon = \frac{2}{22}$

Plugging back we get:

$$\begin{aligned}
 \frac{d \langle m_n \rangle}{dt} &= \alpha \left( \frac{K}{K + \langle p_n \rangle / V} \right)^r + \frac{\alpha r(r+1)}{2K^2 V^2} \left( \frac{K}{K + \langle p_n \rangle / V} \right)^{(r+2)} \sigma_{pn}^2 - \gamma_m \langle m_n \rangle \\
 \frac{d \langle m_c \rangle}{dt} &= \gamma_m \langle m_n \rangle - \mu_m \langle m_c \rangle + \mu_s m_s \\
 \frac{d \langle p_c \rangle}{dt} &= \beta \langle m_c \rangle - \gamma_p \langle p_c \rangle \\
 \frac{d \langle p_n \rangle}{dt} &= \gamma_p \langle p_c \rangle - \delta_p \langle p_n \rangle \\
 \frac{d \langle m_s \rangle}{dt} &= N_c \mu_c \langle m_c \rangle - N_c \mu_s m_s - N_c \delta_m m_s.
 \end{aligned}$$

#### 4.1 Behavior of $m_s$

We have hopes of further reducing this equation set by considering the last equation. Take  $\mu_c = \epsilon + \delta_m, \mu_s = \epsilon$ , then:

$$\frac{dm_s}{dt} = N_c(\epsilon + \delta_m) \langle m_c \rangle - N_c \epsilon m_s - N_c \delta_m m_s = N_c(\epsilon + \delta_m)(\langle m_c \rangle - m_s)$$

For  $N_c \gg 1$ ,  $\langle m_c \rangle - m_s \sim O(\langle m_c \rangle)$ ,  $\frac{dm_s}{dt} \sim N_c O(\nu \langle m_c \rangle) \gg O(\nu \langle m_c \rangle) \sim \frac{d \langle m_c \rangle}{dt}$ . So  $\frac{d \langle m_c \rangle}{dt}$  is adiabatic compared to  $\frac{dm_s}{dt}$  and:

$$\frac{d(m_s - \langle m_c \rangle)}{dt} \approx \frac{dm_s}{dt} = N_c(\epsilon + \delta_m)(\langle m_c \rangle - m_s).$$

Then solving with respect to  $(m_s - \langle m_c \rangle)$ , we get  $m_s - \langle m_c \rangle = (m_s^0 - \langle m_c^0 \rangle) e^{-N_c(\epsilon + \delta_m)t}$ . So for  $t > 0$ , we quickly have

$$m_s - \langle m_c \rangle \ll (m_s^0 - \langle m_c^0 \rangle) \Rightarrow m_s = \langle m_c \rangle.$$

In **figure 12**, we can see  $m_s$  quickly converging to  $\langle m_c \rangle$  within an hour after the simulation starts.

Plugging this result back gives:

$$\begin{aligned}
\frac{d \langle m_n \rangle}{dt} &= \alpha \left( \frac{K}{K + \langle p_n \rangle / V} \right)^r + \frac{\alpha r(r+1)}{2K^2V^2} \left( \frac{K}{K + \langle p_n \rangle / V} \right)^{(r+2)} \sigma_{pn}^2 - \gamma_m \langle m_n \rangle \\
\frac{d \langle m_c \rangle}{dt} &= \gamma_m \langle m_n \rangle - \mu_m \langle m_c \rangle + \mu_s \langle m_c \rangle \\
\frac{d \langle p_c \rangle}{dt} &= \beta \langle m_c \rangle - \gamma_p \langle p_c \rangle \\
\frac{d \langle p_n \rangle}{dt} &= \gamma_p \langle p_c \rangle - \delta_p \langle p_n \rangle
\end{aligned}$$

Notice that this is just the same equation of motion of a single cell, with an additional term that depends on the standard deviation of  $p_n^i$ , which is an **extra dynamic variable** describing the system state. When  $\sigma_{pn}$  goes to 0, **it is guaranteed that the mean dynamics differential equations converge to that of the cellular dynamics of a single cell and will behave collectively like one.**

For  $\sigma_{pn}^2 \neq 0$ , we have new critical point of  $p_n$  satisfying:

$$\alpha\beta \left( \frac{K}{K + \langle p_n \rangle / V} \right)^r \left( 1 + \frac{\sigma_{pn}^2 r(r+1)}{2K^2V^2} \left( \frac{K}{K + \langle p_n \rangle / V} \right)^2 \right) = \delta_m \delta_p \langle p_n \rangle,$$

which yields critical point  $\langle p_n \rangle_0 > p_{n0}$ . For first order approximation of the non-linear terms in  $\frac{d \langle m_n \rangle}{dt}$ ,

$$\begin{aligned}
&\frac{\partial}{\partial \langle p_n \rangle} \left( \alpha \left( \frac{K}{K + \langle p_n \rangle / V} \right)^r + \frac{\alpha r(r+1)}{2V^2K^2} \left( \frac{K}{K + \langle p_n \rangle / V} \right)^{(r-2)} \sigma_{pn}^2 \right) \\
&= -\frac{\alpha r}{KV} \left( \frac{K}{K + \langle p_n \rangle_0 / V} \right)^{r+1} - \frac{\alpha r(r+1)(r+2)\sigma_{pn}^2}{2V^3K^3} \left( \frac{K}{K + \langle p_n \rangle_0 / V} \right)^{r+2} \equiv -a_1
\end{aligned}$$

So

$$a_1 = \frac{\delta_m \delta_p r}{\beta} \frac{\langle p_n \rangle_0 / V}{K + \langle p_n \rangle_0 / V} + \frac{\alpha r(r+1)}{(VK)^3} \left( \frac{K}{K + \langle p_n \rangle_0 / V} \right)^{r+2}.$$

Note that  $a_1 > a$ . With the same linear perturbation around the equilibrium as given in section 2, we have for  $G$ :

$$G_1 = \frac{a_1 \beta}{\nu^2} > \frac{a \beta}{\nu^2} = G,$$

then eigenvalues of the mean system will have positive real parts instead of 0 for the single cell case. This implies instability and a growing amplitude of oscillation. We can also see that as  $\sigma_{pn}^2$  decreases at the beginning, it brings the critical point of the oscillation downwards from the original increased value, and the orbit of  $\langle S \rangle$  simultaneously draws downward, before the amplitude increases and stabilizes as  $\sigma_{pn}$  converges to 0.

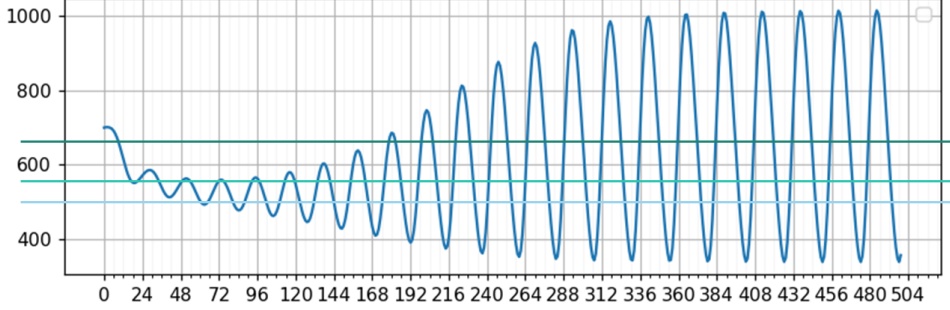


Figure 13:  $\langle p_n \rangle$  vs  $t$  (blue),  $N_c = 100, \nu = \frac{2\pi}{22}, \epsilon = \frac{2}{22}, V = 0.1$ . Horizontal lines mark the decreasing critical values of  $\langle p_n \rangle$ .

## 4.2 Behavior of $\sigma_{pn}^2$

The above arguments justifies  $\sigma_{pn}$  as a measure of synchronization. Plugging in  $m_s = \langle m_c \rangle$  into the single cell differential equations, we get:

$$\begin{aligned} \frac{dm_n^i}{dt} &= \alpha \left( \frac{K}{K + \frac{p_n^i}{V}} \right)^r - \gamma_m m_n^i \\ \frac{dm_c^i}{dt} &= \gamma_m m_n^i - \delta_m m_c^i + \epsilon(\langle m_c \rangle - m_c^i) \\ \frac{dp_c^i}{dt} &= \beta m_c^i - \gamma_p p_c^i \\ \frac{dp_n^i}{dt} &= \gamma_p p_c^i - \delta_p p_n^i, \end{aligned}$$

note that the term  $\epsilon(\langle m_c \rangle - m_c^i)$  is driving the synchronization. As  $\langle m_c \rangle - m_c^i$  goes to 0, the cellular dynamics of each individual cells stabilize to their original periodicity. If we apply variation of constants while ignoring the non-linearity in the first equation, we shall obtain

$$m_c^i - \langle m_c \rangle \sim (m_c^{i0} - \langle m_c \rangle^0) e^{-\epsilon t},$$

with which we can estimate that

$$p_n^i - \langle p_n \rangle \sim (p_n^{i0} - \langle p_n \rangle^0) e^{-\epsilon t},$$

which gives that  $\sigma_{pn} \sim \sigma_{pn}^0 e^{-\epsilon t}$ . In simulations of 100 cell systems, with different parameters given, we can experimentally determine that

$$\sigma_{pn} \sim \sigma_{pn}^0 e^{-0.173\epsilon t}.$$

While there are not yet theoretical justifications for this synchronization coefficient  $-0.173$ , it has worked for different choices of  $\nu$  and  $\epsilon$  (**figure 15, 16, 17**). A potential approach would be to use the full variation of constants by matrices on the perturbation region of  $S$ .

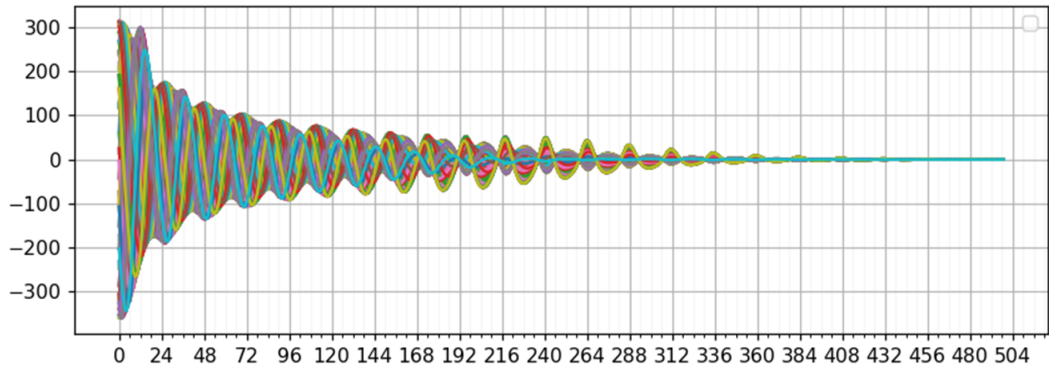


Figure 14:  $p_n^i - \langle p_n \rangle$  vs  $t$  in an 100 cell simulation, with  $\nu = \frac{2\pi}{22}$ ,  $\epsilon = \frac{2}{22}$ ,  $V = 0.1$

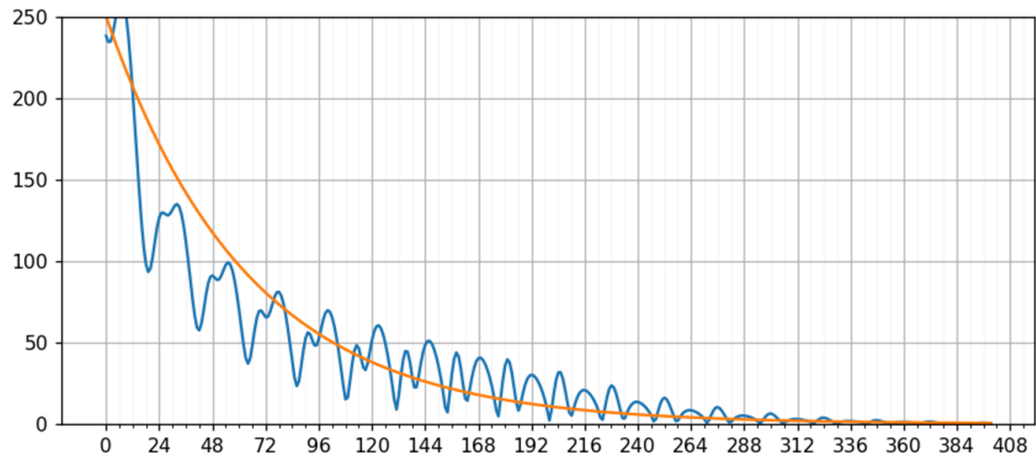


Figure 15:  $\sigma_{pn}$  vs  $t$  in 100 cell simulation, with with  $\nu = \frac{2\pi}{22}$ ,  $\epsilon = \frac{2}{22}$ ,  $V = 0.1$ ;  $250e^{-0.173\epsilon t}$  (orange)

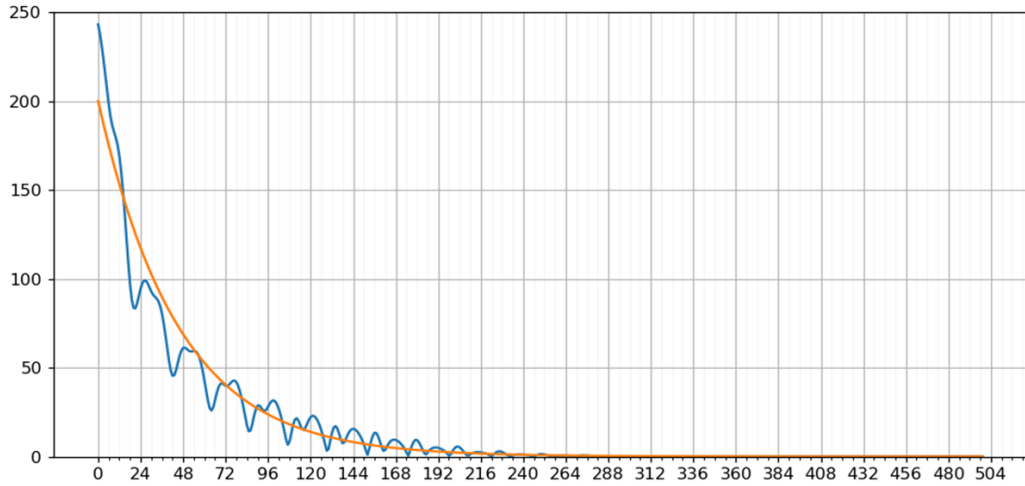


Figure 16:  $\sigma_{pn}$  vs  $t$  in 100 cell simulation (blue), with with  $\nu = \frac{2\pi}{22}$ ,  $\epsilon = \frac{3}{20}$ ,  $V = 0.1$ ;  $250e^{-0.173\epsilon t}$  (orange)

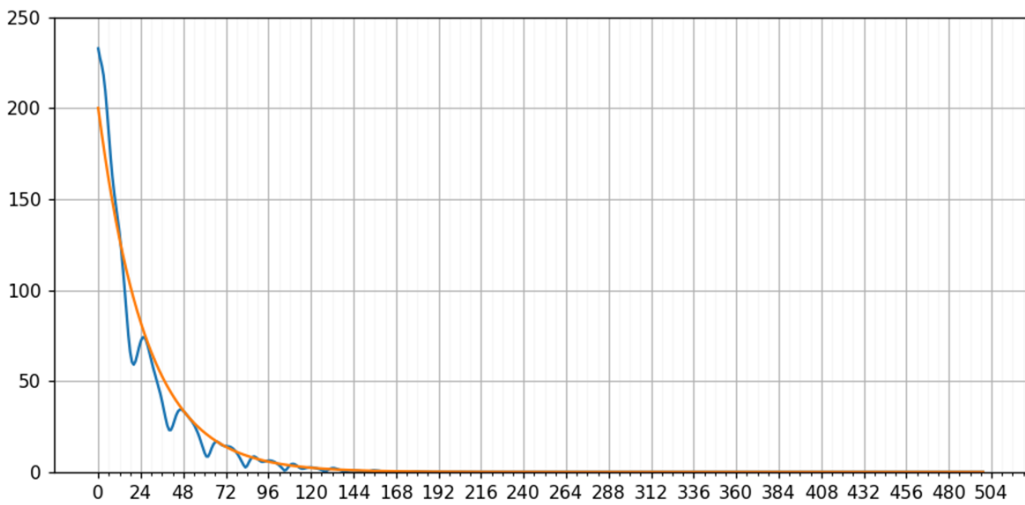


Figure 17:  $\sigma_{pn}$  vs  $t$  in 100 cell simulation (blue), with with  $\nu = \frac{2\pi}{22}$ ,  $\epsilon = \frac{5}{20}$ ,  $V = 0.1$ ;  $250e^{-0.173\epsilon t}$  (orange)

## 5 Conclusion

In this paper I have expanded the single cell to multiple cell model acting as an interactive system, by introducing a blood stream and an exchange rate  $\epsilon$  that is relatively small compared to the other diffusion rates  $\gamma_m, \gamma_p$ , etc. Simulations of this system show strong trends toward synchronization for large number of interacting cells. I also re-expressed the  $(4N+1)$  differential equations governing the multi cell system by a simpler set of 4 involving the mean quantities of the systems and an additional standard deviation term (spread) of cytoplasm concentrations of the protein species across cells. This allows one to make qualitative conclusions about the dynamics of the averages of the cellular quantities, and hence their collective behavior. I provided a heuristic argument for the values of  $\sigma_{pn}$  evolving through time, and experimentally determined it to decay by a factor of  $e^{-0.173\epsilon t}$ .

## References

- [1] Guanyu Wang, Charles S. Peskin, *Entrainment of a cellular circadian oscillator by light in the presence of molecular noise* (2018), Phys. Rev. E 97, 062416, <https://journals.aps.org/pre/pdf/10.1103/PhysRevE.97.062416>.